

# Kinetic analysis of ligand interaction with the gonococcal transferrin-iron acquisition system

Amanda J. DeRocco · Mary Kate Yost-Daljev ·  
Christopher D. Kenney · Cynthia Nau Cornelissen

Received: 15 August 2008 / Accepted: 7 November 2008 / Published online: 2 December 2008  
© Springer Science+Business Media, LLC. 2008

**Abstract** The transferrin iron acquisition system of *Neisseria gonorrhoeae* consists of two dissimilar transferrin binding proteins (Tbp) A and B. TbpA is a TonB dependent transporter while TbpB is a lipoprotein that makes iron acquisition from transferrin (Tf) more efficient. In an attempt to further define the individual roles of these receptors in the process of Tf-iron acquisition, the kinetics of the receptor proteins in regards to ligand association and dissociation were evaluated. Tf association with TbpB was rapid as compared to TbpA. Tf dissociation from the wild-type receptor occurred in a biphasic manner; an initial rapid release was followed by a slower

dissociation over time. Both TbpA and TbpB demonstrated a two-phase release pattern; however, TbpA required both TonB and TbpB for efficient Tf dissociation from the cell surface. The roles of TbpA and TbpB in Tf dissociation were further examined, utilizing previously created HA fusion proteins. Using a Tf-utilization deficient TbpA-HA mutant, we concluded that the slower rate of ligand dissociation demonstrated by the wild-type transporter was a function of successful iron internalization. Insertion into the C-terminus of TbpB decreased the rate of Tf dissociation, while insertion into the N-terminus had no effect on this process. From these studies, we propose that TbpA and TbpB function synergistically during the process of Tf iron acquisition and that TbpB makes the process of Tf-iron acquisition more efficient at least in part by affecting association and dissociation of Tf from the cell surface.

---

A. J. DeRocco · M. K. Yost-Daljev ·  
C. N. Cornelissen (✉)  
Departments of Microbiology and Immunology,  
Virginia Commonwealth University Medical Center,  
P.O. Box 980678, Richmond, VA 23298-0678, USA  
e-mail: cncornel@vcu.edu

**Present Address:**  
M. K. Yost-Daljev  
Division of Consolidated Laboratory Services,  
Richmond, VA, USA

C. D. Kenney  
Departments of Microbiology and Pathology, Virginia  
Commonwealth University Medical Center, Richmond,  
VA 23298-0678, USA

**Present Address:**  
C. D. Kenney  
University of Chicago Medical Center, Chicago, IL, USA

**Keywords** *Neisseria* · TonB · Transferrin · Receptor

## Introduction

*Neisseria gonorrhoeae* is the causative agent of the sexually transmitted disease gonorrhea. *N. gonorrhoeae* is an obligate human pathogen, for which iron is essential to survival. The human host represents an extremely iron limiting environment and consequently, *N. gonorrhoeae* has developed high-affinity

iron acquisition systems to overcome this nutrient deficit. Specifically, this bacterium utilizes host iron-binding proteins, including transferrin (Tf), lactoferrin and hemoglobin (Mickelsen et al. 1982; Schryvers and Morris 1988; Lewis and Dyer 1995).

The gonococcal Tf-iron acquisition system is comprised of two Tf binding proteins, TbpA and TbpB. TbpA is an outer membrane TonB-dependent receptor, providing the pore through which iron is translocated into the cell (Cornelissen et al. 1992). TbpA is necessary for the acquisition of iron from Tf, utilizing TonB-derived energy for this process (Cornelissen et al. 1992). In contrast, TbpB is a surface exposed lipoprotein (Irwin et al. 1993; Lissolo et al. 1995; Cornelissen and Sparling 1996; Renauld-Mongenie et al. 1997; DeRocco and Cornelissen 2007) that is not essential for Tf iron acquisition; however, TbpB makes this process more efficient (Anderson et al. 1994).

TbpA is homologous to other TonB-dependent receptors, such as FepA and FhuA of *Escherichia coli* (Cornelissen et al. 1992). The most N-terminal region of similarity between these receptors is the “TonB box”, located within the plug domain, which has been shown to be the point of interaction between TonB and the outer membrane protein (Gudmundsdottir et al. 1989; Larsen et al. 1997; Cadieux and Kadner 1999; Kenney and Cornelissen 2002). It was previously demonstrated that TbpA and TonB form a stable complex, independent of Tf (Kenney and Cornelissen 2002). Conversely, TbpB did not interact with TonB, demonstrating the specificity of the TbpA–TonB complex (Kenney and Cornelissen 2002).

TbpB contains two detectable Tf binding sites, one located in each of the amino-terminal and carboxy-terminal lobes (Renauld-Mongenie et al. 1997; Retzer et al. 1999; DeRocco and Cornelissen 2007). This finding, along with the internal homology observed between the halves of TbpB, has led to the conclusion that this protein adopts a bi-lobed conformation similar to that of human Tf (Mazarin et al. 1995; Retzer et al. 1998). Several attributes have been linked to the N-lobe of TbpB. This region contains the high-affinity binding domain, which is resistant to denaturation (Vonder Haar et al. 1994; Cornelissen et al. 1997a) and by itself can select the optimum species-specific ligand (Renauld-Mongenie et al. 1997; Retzer et al. 1998). Although the C-lobe is necessary to achieve wild-type function (DeRocco

and Cornelissen 2007), it is unclear what specific role this domain of TbpB plays in the process of Tf-iron acquisition.

Interaction between TbpA and TbpB has not been well defined. The presence of TbpB increases the efficiency of TbpA to internalize iron from Tf, suggesting these two proteins interact, or at least function synergistically on the cell surface (Anderson et al. 1994). The Tf-iron acquisition system demonstrates specificity for holo-Tf. Preferential binding of the optimum ligand is due to the ability of TbpB to discriminate between apo- and holo-Tf (Cornelissen and Sparling 1996). In contrast, TbpA does not demonstrate ligand specificity, interacting with both holo- and apo-Tf (Cornelissen and Sparling 1996). It has also been demonstrated that the presence of TbpB can compensate for a Tf utilization-deficient TbpA mutant, resulting in restored transporter function (Yost-Daljev and Cornelissen 2004; DeRocco and Cornelissen 2007; Noto and Cornelissen 2008). Additionally, the protease accessibility of TbpB is dependent upon the expression of an energized TbpA (Cornelissen et al. 1997a, b). Furthermore, the ligand binding characteristics of the wild-type system (TbpA and TbpB) is distinct, not a result of combining the individual receptors, suggesting that TbpA and TbpB form a unique binding conformation (Cornelissen and Sparling 1996). Taken together, these data support the hypothesis that TbpA and TbpB function together on the cell surface to achieve the wild-type Tf-iron acquisition system.

The kinetics of ligand association with and dissociation from the Tf iron acquisition system are poorly understood. Little is known about the individual contributions of the system components (TbpA, TbpB and TonB) to the overall kinetics of the system. Cornelissen et al. (1997b) demonstrated that the energization state of the Tf-iron acquisition system is important for ligand release, as only 30% of Tf dissociates in TonB-deficient mutants. In *N. meningitidis*, the importance of lipid-modified receptors such as TbpB has been reported, as in their absence ligand does not fully dissociate from the cell surface (Rohde and Dyer 2004). Collectively, these studies indicate that each component of the Tf-iron acquisition system plays a key role in ligand binding kinetics. In an attempt to further define the individual contributions of each protein involved in this high-affinity iron acquisition system, we examined the

kinetics of Tf association with and dissociation from the cell surface.

## Materials and methods

### Strains and media

The strains utilized for this study are listed in Table 1. Gonococci were grown on GC medium base (Difco),

with Kellogg's supplement 1 (Kellogg et al. 1963) and 12  $\mu\text{M}$   $\text{Fe}(\text{NO}_3)_3$ . GC agar was supplemented with 10  $\mu\text{g}/\text{ml}$  of gentamycin for selection of gonococcal transformants. The gonococci were grown in a liquid chelexed defined medium (CDM) (West and Sparling 1987) to achieve iron-stressed conditions. All gonococcal strains were cultivated at 37°C in 5%  $\text{CO}_2$ . Plasmids were propagated in *E. coli* strain Top10 (Table 1), which was grown in LB broth (Bertani 1951, 2004) with 50  $\mu\text{g}/\text{ml}$  of kanamycin.

**Table 1** *Escherichia coli* and *Neisseria gonorrhoeae* Strains

Strain	Phenotype (genotype)	Reference/source
<i>E. coli</i>		
TOP10	F- <i>mcrA</i> $\Delta$ ( <i>mrr-hsdRMS-mcrBC</i> ) $\Phi$ 80 <i>lacZ</i> $\Delta$ <i>M15</i> $\Delta$ <i>lacX74</i> <i>recA1</i> <i>deoR</i> <i>araD139</i> $\Delta$ ( <i>ara-leu</i> ) 7697 <i>galU galK rpsL</i> (Str <sup>R</sup> ) <i>endA1 nupG</i>	Invitrogen
<i>N. gonorrhoeae</i> strains <sup>a</sup>		
FA19	Wild type	Mickelsen and Sparling (1981)
FA6747	TbpA <sup>−</sup> ( <i>tbpA::mTn3cat</i> )	Cornelissen et al. (1992)
FA6905	TbpB <sup>−</sup> ( $\Delta$ <i>tbpB</i> )	Cornelissen and Sparling (1996)
FA6935	TonB box ( <i>tbpA</i> I <sub>16</sub> P)	Cornelissen et al. (1997b)
MCV516	L9HA TbpA, Lbp <sup>−</sup> ( <i>tbpA</i> $\nabla$ HA, $\Delta$ <i>tbpB</i> , <i>lbp::</i> $\Omega$ )	Yost-Daljev and Cornelissen (2004)
MCV612	TbpB <sup>−</sup> , Ton <sup>−</sup> ( $\Delta$ <i>tbpB</i> , <i>tonB::</i> $\Omega$ )	This study
MCV613	TbpA <sup>−</sup> , Ton <sup>−</sup> ( <i>tbpA::mTn3</i> , <i>tonB::</i> $\Omega$ )	This study
MCV803	HA1 <sub>(37)</sub> TbpB, TbpA <sup>−</sup> , Lbp <sup>−</sup> ( <i>tbpB</i> $\nabla$ HA, <i>tbpA::mTn3</i> , <i>lbp::</i> $\Omega$ )	DeRocco and Cornelissen (2007)
MCV804	HA2 <sub>(97)</sub> TbpB, TbpA <sup>−</sup> , Lbp <sup>−</sup> ( <i>tbpB</i> $\nabla$ HA, <i>tbpA::mTn3</i> , <i>lbp::</i> $\Omega$ )	DeRocco and Cornelissen (2007)
MCV813	HA3 <sub>(175)</sub> TbpB, TbpA <sup>−</sup> , Lbp <sup>−</sup> ( <i>tbpB</i> $\nabla$ HA, <i>tbpA::mTn3</i> , <i>lbp::</i> $\Omega$ )	DeRocco and Cornelissen (2007)
MCV815	HA4 <sub>(293)</sub> TbpB, TbpA <sup>−</sup> , Lbp <sup>−</sup> ( <i>tbpB</i> $\nabla$ HA, <i>tbpA::mTn3</i> , <i>lbp::</i> $\Omega$ )	DeRocco and Cornelissen (2007)
MCV817	HA5 <sub>(327)</sub> TbpB, TbpA <sup>−</sup> , Lbp <sup>−</sup> ( <i>tbpB</i> $\nabla$ HA, <i>tbpA::mTn3</i> , <i>lbp::</i> $\Omega$ )	DeRocco and Cornelissen (2007)
MCV819	HA6 <sub>(424)</sub> TbpB, TbpA <sup>−</sup> , Lbp <sup>−</sup> ( <i>tbpB</i> $\nabla$ HA, <i>tbpA::mTn3</i> , <i>lbp::</i> $\Omega$ )	DeRocco and Cornelissen (2007)
MCV821	HA7 <sub>(453)</sub> TbpB, TbpA <sup>−</sup> , Lbp <sup>−</sup> ( <i>tbpB</i> $\nabla$ HA, <i>tbpA::mTn3</i> , <i>lbp::</i> $\Omega$ )	DeRocco and Cornelissen (2007)
MCV823	HA8 <sub>(607)</sub> TbpB, TbpA <sup>−</sup> , Lbp <sup>−</sup> ( <i>tbpB</i> $\nabla$ HA, <i>tbpA::mTn3</i> , <i>lbp::</i> $\Omega$ )	DeRocco and Cornelissen (2007)
MCV825	HA9 <sub>(660)</sub> TbpB, TbpA <sup>−</sup> , Lbp <sup>−</sup> ( <i>tbpB</i> $\nabla$ HA, <i>tbpA::mTn3</i> , <i>lbp::</i> $\Omega$ )	DeRocco and Cornelissen (2007)
Plasmid		
pVCU691	Description pCR2.1 containing <i>tonB::</i> $\Omega$	Kenney and Cornelissen (2002)

<sup>a</sup> Phenotype listed includes position of the last amino acid prior to HA insertion (parentheses). Residues are numbered starting from the first amino acid in the mature protein

### Construction of TonB mutants

The TonB<sup>−</sup> strains MCV612 and MCV613 were constructed by insertion of a gentamycin resistance-encoding  $\Omega$  cassette into the *tonB* gene of strains FA6905 and FA6747, respectively. FA6905 and FA6747 were transformed with the linearized plasmid pVCU691 as described previously (Kenney and Cornelissen 2002). The resulting transformants were selected for growth on gentamycin-containing media and screened by Western blot for the absence of TonB.

### Human transferrin iodination

Iodination of holo-Tf was performed as described previously (Cornelissen et al. 1997b). Briefly, 100% saturated human Tf solution was mixed with Na<sup>125</sup>I (Perkin Elmer) in an Iodogen-coated tube (Pierce) according to manufacturer's recommendations. To separate <sup>125</sup>I from the iodinated Tf, the mixture was passed over a desalting column (Pierce). The concentration of <sup>125</sup>I labeled Tf was then determined by BCA assay (Pierce).

### Ligand association analysis

To examine ligand association with the cell surface, gonococci were grown under iron stressed conditions. After 3 h of growth, 100  $\mu$ l of culture was added to each well of a Millipore Multiscreen microtiter plate. Gonococci were incubated with 10 nM <sup>125</sup>I-Tf for 1, 2, 3, 5, 10, and 20 min. Non-specific binding was determined by the addition of excess unlabeled competitor (3.6  $\mu$ M). Following incubation, unbound Tf was removed by filtration. The wells were washed, dried, removed from the plate and counted with a Packard Cobra 5005 gamma counter. Counts per minute (CPM) were averaged and the non-specific counts subtracted. Specific CPM was converted to nanograms of Tf bound over time using the specific activity of the <sup>125</sup>I-Tf preparation. The values reported are a percentage of the total, maximal binding.

### Ligand dissociation analysis and determination of $k_{\text{off}}$

To examine ligand dissociation, release assays were performed as described previously (Cornelissen et al.

1997b). Gonococci were grown under iron stressed conditions. After 3 h of growth, 100  $\mu$ l of culture was added to each well of a Millipore Multiscreen microtiter plate. <sup>125</sup>I-Tf was added to each well at a final concentration of 100 nM and allowed to bind for 20 min at room temperature. Excess unlabelled 100% saturated Tf (3.6  $\mu$ M) was added at 1, 5, 10, 20, and 40 min. Cells incubated with <sup>125</sup>I-Tf in the absence of competitor represented the total amount bound by each strain. To calculate the non-specific binding, excess unlabelled Tf was added to wells in parallel for the duration of the assay. Following incubation, unbound Tf was removed by filtration. The wells were washed, dried, removed from the plate and counted with a Packard Cobra 5005 gamma counter. Counts per minute were averaged and the non-specific counts subtracted. Specific CPM were converted to nanograms of Tf bound over time using the specific activity of the <sup>125</sup>I-Tf preparation.

To calculate the off-rate ( $k_{\text{off}}$ ) for each strain, specific CPM values were log transformed. Linear regression was performed in order to calculate the slope of the line, representing  $-k_{\text{off}}$ . For comparison between strains, individual experiments were plotted for each strain, the mean of the slopes was determined, and the standard deviation was calculated. The ligand half-life for each binding site was calculated from the reported off-rate using the following equation:  $\ln(2)/k_{\text{off}}$ .

### Equilibrium phase binding assay

To determine the binding affinity and capacity of the TbpB-HA fusion strains an equilibrium phase Tf binding assay was performed as described previously (Cornelissen and Sparling 1996). Iron stressed gonococci were grown for 3 h and 100  $\mu$ l of culture were added to each well of a Millipore Multiscreen microtiter plate (Millipore). The bacteria were mixed with various concentrations of 100% saturated <sup>125</sup>I-Tf (3–100 nM) and allowed to incubate at room temperature for 20 min. Following incubation, the plates were filtered to remove unbound <sup>125</sup>I-Tf and each well was washed, dried, removed and counted with a Packard Cobra 5005 gamma counter. Non-specific binding for each concentration of <sup>125</sup>I-Tf was determined by the addition of excess (3.6  $\mu$ M) unlabeled competitor. The non-specific counts were subtracted from each condition to obtain specific binding values.

Specific CPM was converted to nanograms of Tf bound using the specific activity of the  $^{125}\text{I}$ -Tf preparation. The amount of  $^{125}\text{I}$ -Tf bound was standardized to total cellular protein, which was determined by BCA assay.

To calculate the Tf binding affinity for each strain, nanograms of Tf bound at each concentration of ligand was determined and the mean of at least three assays was plotted. Non-linear regression analysis utilizing a single binding-site hyperbola (GraphPad Prism 4.0 software) generated a best-fit line, from which  $B_{\text{max}}$  and  $K_d$  (affinity constant) values for each strain were determined. Capacity, the number of binding sites per  $\mu\text{g}$  of protein, was calculated from the  $B_{\text{max}}$  value.

### Statistical analysis

Statistical significance was determined using a two-tailed, unpaired Student's *t*-test in which a *P* value of  $\leq 0.05$  was considered significant.

## Results

Transferrin association with receptor components on the cell surface is differentially impacted by the Ton system

Transferrin association with the wild-type strain and mutants lacking individual components of the Tf-iron acquisition system was examined. Whole, iron-stressed gonococci were incubated with  $^{125}\text{I}$ -Tf for 1–20 min and the amount of Tf bound over time was determined. In order to examine the role of the Ton system in ligand association with the cell surface, the previously described “TonB box” mutant, FA6935, was utilized (Table 1). This strain contains a point mutation in the “TonB box” of TbpA, inhibiting the interaction of TonB with the receptor (Cornelissen et al. 1997b). Transferrin association with the wild-type (FA19) and the “TonB box” mutant (FA6935) are shown in Fig. 1a. A single phase association curve was apparent, indicating that the surface-exposed components of the system (TbpA and TbpB) work synergistically to bind Tf. The association of Tf with the cell surface was not TonB dependent, as evidenced by the overlapping curves of FA19 and FA6935 (Fig. 1a). Approximately 60% of the ligand

was bound to the cell surface within 1 min, with maximum binding achieved by 10 min.

Analysis of ligand association with the individual Tf-iron acquisition system components was performed (Fig. 1b, c). To decipher the role of TonB energy in this process, two TonB<sup>−</sup> strains were created: MCV612 (TbpB<sup>−</sup>, TonB<sup>−</sup>) and MCV613 (TbpA<sup>−</sup>, TonB<sup>−</sup>) (Table 1). When expressed independently, Tf associated with TbpA more slowly than with the wild-type system, as only 50% of ligand associated after 1 min, reaching maximum binding by 20 min (Fig. 1b). Interestingly, ligand association with TbpA was impacted by the absence of TonB (Fig. 1b). MCV612 demonstrated a slowed initial association, with only 20% bound in the first minute. However, at later time points, this de-energized strain resembled the parental control FA6905, binding 80% of Tf at 10 min and reaching maximum binding by 20 min (Fig. 1b). In contrast, Tf binding to TbpB was not dependent on TonB, as the association curves of both FA6747 (parent strain) and MCV613 (TonB<sup>−</sup>) overlapped (Fig. 1c). Transferrin rapidly associated with a strain expressing TbpB only; 90% of the ligand bound in the first minute and the reaction reached 100% binding within 2 min (Fig. 1c). The individual receptors demonstrated differential binding characteristics when expressed independently; TbpB facilitated more efficient association and TonB was required for effective Tf association with TbpA. Overall, these results suggest that the receptor components of the Tf iron acquisition system function synergistically to allow Tf association with the cell surface.

In the wild-type system, TbpB is necessary to rapidly dissociate transferrin from the cell surface

To examine ligand dissociation from the cell surface whole iron-stressed gonococci were incubated with  $^{125}\text{I}$  labeled Tf for 20 min and excess unlabeled Tf was then added for specific time periods. The dissociation rate constant ( $k_{\text{off}}$ ) and ligand half-life were calculated from these experiments. The wild-type strain demonstrated a biphasic release pattern; an initial, rapid dissociation followed by a slower release over time (Fig. 2a). Within 1 min, 50% of the ligand was released from the cell surface and by 40 min, little, if any Tf remained bound (Fig. 2a). The phase-one, or the initial release, from FA19

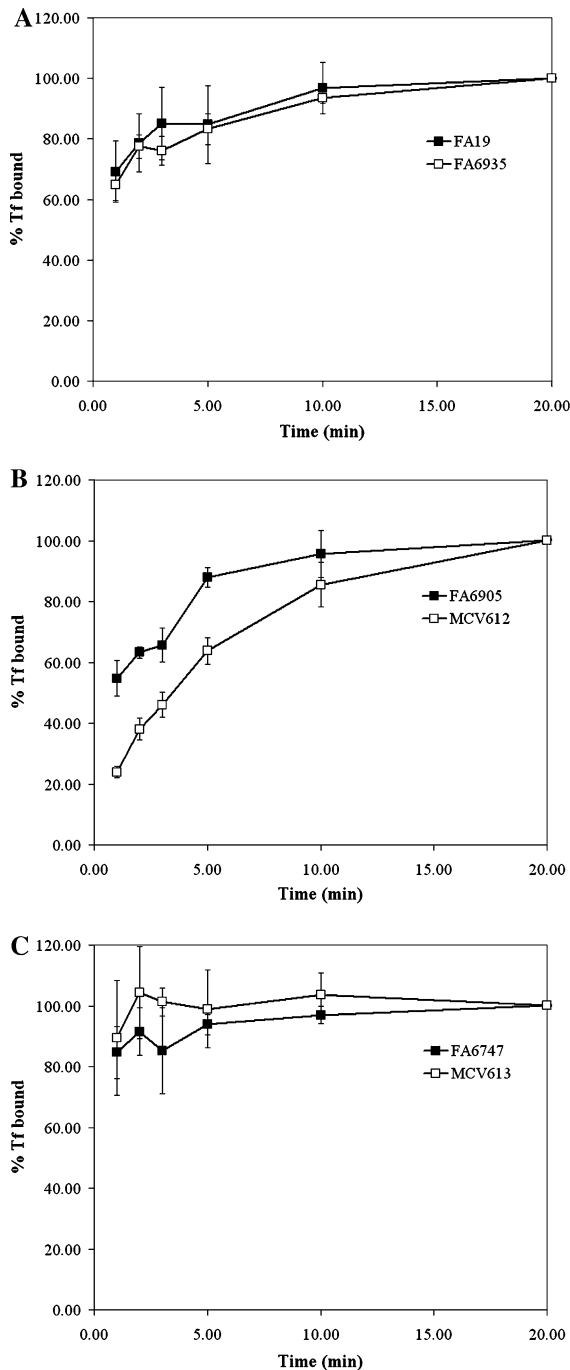


**Fig. 1** Transferrin association with the cell surface in the presence and absence of TonB-derived energy. Whole, iron-stressed gonococci were incubated with  $^{125}$ I-Tf for various periods of time. The amount of Tf bound at each time point was determined and values are expressed as a percentage of the maximum amount of Tf bound by each strain. The wild type system, expressing both TbpA and TbpB is shown in *Panel A*. *Panel B* depicts the TbpA-only strains and *Panel C* represents the TbpB-only strains. In each *panel*, strains containing TonB are denoted by the *closed symbols* and strains unable to energize the Tbp components are denoted by the *open symbols*. Standard deviations are represented by *error bars*

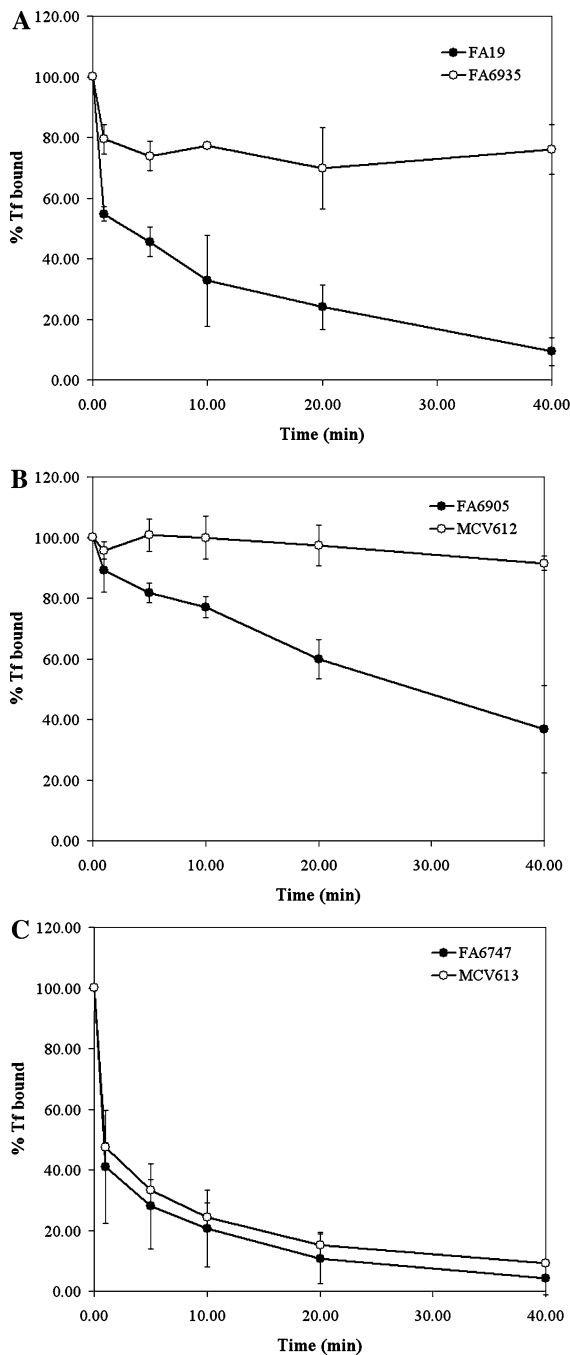
previous studies, FA6935 released only 20% of the bound Tf over the course of the experiment (Cornelissen et al. 1997b) (Fig. 2a). The initial, rapid dissociation was only moderately impacted in this strain, demonstrating a ligand half-life of 3.4 min, and implying that the first phase of Tf release was not energy dependent (Fig. 2a). In contrast, the “TonB box” mutation dramatically impacted ligand release, causing a greater than 20-fold increase in ligand half-life (Table 2).

In the absence of TbpB, TbpA also demonstrated biphasic ligand dissociation from the cell surface (Fig. 2b). However, only 60% of the total ligand was released over 40 min, implicating the importance of TbpB in complete Tf dissociation from the cell surface (Fig. 2b). The initial release from TbpA was slower than that seen with FA19, with a half-life of 6.9 min. The corresponding phase-two half-life for FA6905 was 23.1 min, comparable to that of FA19 and indicating that TbpA was responsible for the slower dissociation seen in the wild-type strain (Table 2). Tf release from TbpA was TonB dependent, as in the absence of TbpB and TonB-derived energy 100% of the ligand remained bound to the cell surface after 40 min (Fig. 2b). The half-life for de-energized TbpA (MCV612) was identical to the phase-two half-life of FA6935 (Table 2). Cumulatively, these results indicate that Tf associates with TbpA in an energy-dependent manner (Fig. 1a), and once bound, this tight protein–protein complex is unlikely to dissociate without TonB-derived energy.

When expressed alone, TbpB also exhibited a biphasic release pattern, suggestive of multiple binding sites or conformations (Fig. 2c). The initial dissociation of Tf from TbpB occurred rapidly, with 60% of the ligand released in 1 min, corresponding to a ligand half-life of 0.7 min. The secondary release phase demonstrated by TbpB exhibited a half-life of

demonstrated a half-life of 1.2 min, while the second, slower phase exhibited a half-life of 13.9 min (Table 2). In contrast to the Tf association experiments, the absence of TonB-derived energy greatly impacted ligand dissociation from the wild-type cell surface (compare Figs. 1a, 2a). In agreement with





11.6 min (Table 2). As expected, the absence of TonB had no effect on the ability of TbpB to release the ligand (Fig. 2c; Table 2). This result implies that the initial, energy-independent release in FA6935 was due to the presence of TbpB (Fig. 2a). Despite the similar off-rates and ligand half-lives exhibited by the wild-type and single mutants, the obviously

**Fig. 2** Transferrin dissociation from the cell surface in the presence and absence of TonB-derived energy. Whole, iron-stressed gonococci were incubated with  $^{125}\text{I}$  labeled transferrin and allowed to bind. Excess unlabeled Tf was then added and incubated for the indicated amounts of time. The amount of radiolabeled Tf remaining at each time point is expressed as a percentage of Tf bound in the absence of competitor (0 min). The wild type system, expressing both TbpA and TbpB is shown in *Panel A*. *Panel B* depicts the TbpA-only strains and *Panel C* represents the TbpB-only strains. In each *panel*, strains containing TonB are denoted by the *closed symbols* and strains unable to energize the Tbp components are denoted by the *open symbols*. Standard deviations are represented by *error bars*

different dissociation trends demonstrated by these strains suggest that when the two receptors are present on the cell surface they function in-concert, rather than independently, to achieve wild-type dissociation. This concept was evident with TbpB, as the slower release rate was not readily detectable in the wild-type dissociation curve. Additionally, the inability of Tf to fully dissociate from TbpA in the absence of TbpB suggests that in the wild-type strain, TbpB functions to rapidly dissociate ligand from the cell surface, indicating that these two receptors function together.

#### The C-terminus of TbpB is required for the rapid release of transferrin from the cell surface

Previous studies have demonstrated that TbpB contains two Tf binding sites, located in the N- and C-lobes of the protein (Renault-Mongenie et al. 1997; Retzer et al. 1999; DeRocco and Cornelissen 2007). These binding sites work together to achieve wild-type function of the protein (DeRocco and Cornelissen 2007); however, due to size constraints, it is unlikely that TbpB binds multiple Tf molecules simultaneously. Instead, these results and those of others, suggest that the two ligand binding domains of TbpB form one binding pocket for Tf. The release trend exhibited by TbpB indicated that two distinct Tf binding sites were detectable and that each was playing a role in ligand release from the receptor (Fig. 2c). In an attempt to further decipher Tf dissociation from TbpB, we utilized the previously created TbpB-HA mutants (DeRocco and Cornelissen 2007) and examined the impacts of mutagenesis on binding kinetics. These analyses were performed in strains lacking TbpA in order to assess the rate of

**Table 2** Calculated off-rate

Strain <sup>a, b</sup>	$k_{\text{off}}$ (min <sup>-1</sup> ) <sup>c</sup> phase 1	Half-life (min) <sup>d</sup> phase 1	$k_{\text{off}}$ (min <sup>-1</sup> ) <sup>c</sup> phase 2	Half-life (min) <sup>d</sup> phase 2
FA19	0.6 ± 0.04	1.2	0.05 ± 0.01	13.9
FA6935	0.2 ± 0.06	3.4	0.002 ± 0.001	346.5
FA6905	0.1 ± 0.08	6.9	0.03 ± 0.01	23.1
MCV612	0.002 ± 0.00	346.5	NA	NA
MCV516 (L9)	0.5 ± 0.21	1.4	0.06 ± 0.03	12.1
<i>Off-rate of TbpB</i>				
FA6747	1.0 ± 0.42	0.7	0.06 ± 0.03	11.6
MCV613	0.8 ± 0.03	0.9	0.04 ± 0.004	17.3
MCV803 (1)	0.7 ± 0.42	1.0	0.07 ± 0.02	9.6
MCV804 (2)	0.9 ± 0.62	0.8	0.07 ± 0.01	10.5
MCV813 (3)	1.2 ± 0.95	0.6	0.05 ± 0.03	13.5
MCV819 (6)	0.5 ± 0.37	1.3	0.07 ± 0.02	10.6
MCV821 (7)	0.4 ± 0.39	1.6	0.06 ± 0.03	11.1
MCV825 (9)	0.3 ± 0.21	2.6	0.05 ± 0.03	13.9

<sup>a</sup> FA19 and FA6905 represent the wild-type and TbpA-only controls, respectively. MCV516 is TbpB<sup>-</sup>

<sup>b</sup> FA6747 represents the TbpB-only control, all strains are TbpA<sup>-</sup>

<sup>c</sup> Off-rate determined from slope of best fit line using GraphPad Prism 4.0 software. Values represent the mean slope of at least three experiments ± standard deviation

<sup>d</sup> Half-life calculated from the average  $k_{\text{off}}$  value

NA Not applicable

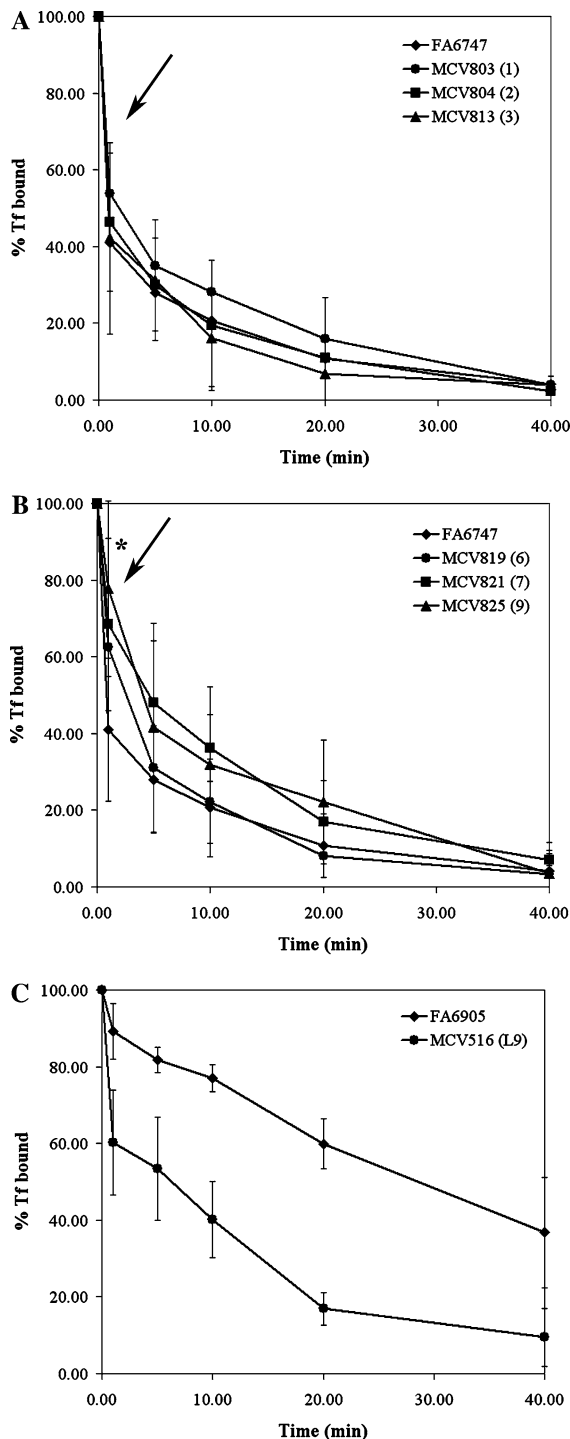
release from TbpB only. The TbpB-HA fusion strains demonstrated a biphasic release pattern similar to that of the parent strain, FA6747 (Fig. 3). The N-terminal insertion mutants (MCV803, MCV804 and MCV813) exhibited release patterns and dissociation constants that were indistinguishable from the parental strain, implying that insertion into these locations did not adversely affect Tf release from TbpB (Fig. 3a; Table 2). However, it was noted that MCV803 (HA3) bound considerably less <sup>125</sup>I-Tf as compared to FA6747 (data not shown). The dissociation curves of the C-terminal mutants (MCV819, MCV821 and MCV825) were different from that of the parental strain (Fig. 3b). In these mutants the initial release was slowed relative to FA6747, with approximately 25–40% of ligand released at 1 min for the HA mutants versus 60% released by the parent strain (Fig. 3b). By statistical analysis, the MCV819 ( $P = 0.02$ ), MCV821 ( $P = 3 \times 10^{-5}$ ) and MCV825 ( $P = 2 \times 10^{-4}$ ) curves were significantly different from FA6747 at the 1 min time point, implicating a role for the C-terminus in the initial rapid release of Tf from TbpB. The C-terminal

mutants MCV819 (HA6) and MCV821 (HA7) exhibited similar dissociation rate constants relative to FA6747, despite the apparently significant decrease in Tf dissociation (Fig. 3b; Table 2). The MCV825 (HA9) strain, however, demonstrated a greater than three-fold decrease in the phase-one ligand half-life when compared to the parent strain (2.6 vs. 0.7 min), implying that the HA insertion had impacted the rate of Tf release (Table 2). No difference was noted in the phase-two dissociation rate constant of this mutant, suggesting that this region had not been impacted by the HA insertion. Collectively these studies demonstrate the importance of the C-terminus in the rapid release of Tf from TbpB.

The affinity of TbpB for Tf is not affected by insertion of the HA epitope

It has been reported previously that TbpB is a high affinity receptor for Tf with a measured  $K_d$  of approximately 10 nM (Cornelissen and Sparling 1996). Utilizing an <sup>125</sup>I-Tf equilibrium phase binding assay to estimate both  $K_d$  and receptor copy number,





the impact of the HA epitope on ligand affinity was examined (Table 3). Scatchard plot analysis of the parent strain revealed a single line, again implying the presence of only one binding site (data not

**Fig. 3** Transferrin dissociation from HA mutants. Whole, iron-stressed gonococci were incubated with  $^{125}\text{I}$  labeled transferrin and allowed to bind. Excess unlabeled Tf was then added to facilitate release of labeled ligand. The amount remaining at each time point is expressed as a percentage of Tf bound in the absence of competitor (0 min). The TbpB-HA N-terminal mutants are shown in *Panel A*. *Panel B* depicts the TbpB-HA C-terminal mutants. FA6747 serves as the parental control, all strains are TbpA<sup>+</sup>. In *panel C*, the utilization-deficient TbpA-HA mutant is depicted. FA6905 serves as the parental control strain, and both strains are TbpB<sup>+</sup>. Curves represent the mean of at least four independent assays. The *solid arrows* indicate the initial rapid release attributed to the C-terminus of TbpB. Strains are listed according to strain name with the location of the HA epitope in *parentheses*. Standard deviations are represented by *error bars*. \*indicates strains are significantly different from the parent ( $P \leq 0.05$ ) at the 1 min time point

shown). This observation suggested that the two Tf-binding domains of TbpB function together to form a single Tf binding pocket.

The N-terminal TbpB-HA fusion strains demonstrated similar affinity constants relative to FA6747 (Table 3). In the case of MCV803 (HA3), this result implied that diminished binding was not a reflection of decreased affinity for Tf (Table 3). However, this strain demonstrated an approximately ten-fold decrease in the number of receptors relative to FA6747. The decrease in the number of functional binding sites corresponds to the diminished  $^{125}\text{I}$ -Tf binding observed in both the ligand dissociation and equilibrium phase assays, implying that the effective number of binding sites in this strain was disrupted by the HA insertion. The C-terminal insertion mutants also showed no change in their apparent  $K_d$  (Table 3).

#### Transferrin completely dissociates from a utilization-deficient TbpA mutant

The TbpA dissociation analysis indicated that the transporter tightly associates with Tf. TbpA provides the pore through which iron, once it has been removed from Tf, is translocated into the cell. To test the hypothesis that the slower ligand dissociation from TbpA occurs as a result of Tf utilization by the cell, a previously created TbpA utilization-deficient mutant (Yost-Daljev and Cornelissen 2004) was examined. An HA insertion was made into the putative loop 9 (L9) of TbpA, generating a mutant that had wild-type affinity for the ligand, but was

**Table 3** Affinity and capacity of TbpB

Strain <sup>a</sup>	$K_d$ (nM) <sup>b</sup>	Capacity <sup>c</sup> (receptors/ $\mu$ g TCP <sup>d</sup> )
FA6747	$14.6 \pm 2.3$	$9.8 \times 10^8$
MCV803 (1)	$12.04 \pm 4.2$	$5.8 \times 10^8$
MCV804 (2)	$15.01 \pm 6.1$	$9.9 \times 10^8$
MCV813 (3)	$6.13 \pm 3.5$	$8.4 \times 10^7$
MCV819 (6)	$10.62 \pm 2.7$	$1.0 \times 10^9$
MCV821 (7)	$14.69 \pm 5.5$	$9.2 \times 10^8$
MCV825 (9)	$18.13 \pm 4.2$	$1.1 \times 10^9$

<sup>a</sup> FA6747 represents the parent strain control, all strains are TbpA<sup>−</sup>

<sup>b</sup>  $K_d$  values calculated by GraphPad Prism 4.0 software and represent the mean of at least three assays  $\pm$  standard deviation

<sup>c</sup> Capacity determined from  $B_{\max}$  values calculated by GraphPad Prism 4.0 software and represent the mean of at least three assays

<sup>d</sup> TCP Total cellular protein determined by bicinchoninic acid (BCA) assay

unable to utilize Tf as a sole iron source (MCV516) (Yost-Daljev and Cornelissen 2004). MCV516 demonstrated a release pattern similar to that of the wild-type strain FA19, despite the absence of TbpB (compare Figs. 2a, 3c). Within 1 min, approximately 40% of the ligand was released, with complete dissociation of Tf by 40 min, corresponding to a ligand half-life of 1.4 and 12.1 min, respectively (Fig. 3c; Table 2). The HA insertion in TbpA dramatically altered the initial release of Tf from the receptor, causing a four-fold increase in ligand half-life. These results indicate that in the absence of iron internalization by TbpA, the first phase of Tf release is exaggerated as compared to the parental strain FA6905.

## Discussion

Transferrin binding and iron utilization by *N. gonorrhoeae* is a complex process involving at least three proteins, TbpA, TbpB and TonB. This process incorporates four steps: Tf binding, removal of iron from Tf, internalization of iron, and release of Tf from the cell surface. TbpA has the ability to complete all four of these steps; however, it requires TonB to accomplish iron internalization and

subsequent Tf release. The methodologies employed in the current study do not allow us to determine whether TonB-derived energy is necessary for removal of iron from Tf.

Examination of Tf association with the wild-type cell surface indicated that both TbpA and TbpB work together to complete this step, as only one phase of Tf association was detected. Cornelissen et al. (1997b) suggested that TbpB undergoes a TbpA-dependent conformational change. Therefore, TbpB may behave differently in the presence of the outer membrane transporter, an hypothesis supported by our association experiments. Tf binding to TbpA was enhanced by the presence of TonB. In contrast, ligand association with the wild-type system, comprised of both proteins, was apparently TonB independent, further supporting the conclusion that both TbpA and TbpB function synergistically during the initial step of Tf-iron acquisition.

The crystal structure of FepA, a TonB-dependent transporter, indicates that the surface exposed loops are disordered, implying flexibility of these domains (Buchanan, Smith et al. 1999). Additionally, it was demonstrated that the loops of FepA move upon binding and transport of the ligand (Klug et al. 1998; Scott et al. 2002). Presumably, TbpA undergoes a similar conformational change to accomplish iron stripping and transport. Insertion into the surface exposed loop 9 of TbpA rendered a utilization-deficient mutant (Yost-Daljev and Cornelissen 2004). Transferrin rapidly and completely dissociated from this strain, in contrast to the parental strain expressing wild-type TbpA. This result implies that the slower off-rates demonstrated by wild-type TbpA may result from internalization of Tf-bound iron.

Tf dissociation from TbpB occurred in a biphasic manner, consistent with the presence of two binding sites. The majority of Tf was released from TbpB rapidly, as approximately 60% dissociated within 1 min. The results from the current study suggested that the C-lobe of TbpB was required for the rapid release of Tf. It has been demonstrated that the C-lobe of Tf specifically associates with the N-lobe of TbpB while the N-lobe of the ligand binds to the C-lobe of TbpB (Retzer et al. 1999; Sims and Schryvers 2003). This binding pattern suggests that each domain of TbpB interacts with a single lobe of Tf (Alcantara and Schryvers 1996), which results in a strengthened interaction between receptor and ligand.

Previous studies have suggested that each half of TbpB wraps around an individual lobe of Tf. Therefore, TbpB undergoes extensive conformational changes upon interaction with the ligand (Retzer et al. 1999). Our results from ligand binding and kinetic studies support this contention, indicating that the two Tf binding sites of TbpB create one binding pocket for the ligand.

The TbpB-HA fusion proteins demonstrated a single binding site with an affinity for Tf of approximately 10 nM, in agreement with previous studies (Cornelissen and Sparling 1996). Three TbpB-HA mutants contain insertions in a Tf binding domain of TbpB: MCV815 (HA4), MCV817 (HA5) and MCV823 (HA8) (DeRocco and Cornelissen 2007). The insertions into MCV815 and MCV816 interrupted the N-terminal Tf binding domain of TbpB, while the insertion in MCV823 has impacted the C-terminal ligand-binding domain (DeRocco and Cornelissen 2007). Under the conditions tested here,  $^{125}\text{I}$ -Tf binding could not be detected in the Tf binding domain mutants (data not shown). Our previous studies indicated that these strains demonstrate reduced but specific binding of Tf in solid phase binding assays (DeRocco and Cornelissen 2007). It has been suggested that the individual domains of TbpB do not bind Tf to the same degree as the wild-type protein (Renauld-Mongenie et al. 1997; Retzer et al. 1999; Krell et al. 2003), implying that each half of TbpB has a much lower affinity for the ligand as compared to the full-length protein. We hypothesize that by interrupting either binding domain in TbpB, the remaining bound Tf could not be detected in the assays used in the current study. In an attempt to address this possibility we increased the ligand incubation time as well the concentration of  $^{125}\text{I}$ -Tf. Despite these alterations, binding was not detected for any of the strains. Lower affinity binding can be difficult to detect using rapid filtration assays as the ligand quickly dissociates during the washing and filtration steps (Jones 1982; Bylund and Yamamura 1990; Jian-Xin Wang et al. 1992). Collectively, these results support the idea that the individual domains of TbpB have a lower affinity for Tf as compared to the full-length protein and therefore both domains are necessary to achieve wild-type levels of binding.

TonB plays a role in the kinetics of Tf binding to TbpA, but does not directly impact TbpB. We

hypothesize that in energizing TbpA, TonB causes a conformational change in the transporter, and by elimination of this interaction TbpA remains static and unable to accomplish iron transport. However, once TbpA interacts with TonB, this receptor can carry out the remaining steps in Tf-iron acquisition. In this model, once TbpA has removed iron from the ligand, TbpA cannot release and bind to another molecule of Tf until iron transport into the periplasm has been accomplished with the participation of TonB.

TbpB is the only non-essential component of the Tf-iron acquisition system. The role of this lipoprotein in Tf utilization has not been completely defined; however, TbpB makes iron uptake from Tf more efficient (Anderson et al. 1994). Our analyses demonstrate that this increase in efficiency is in part due to the ability of TbpB to affect rapid association and dissociation of Tf with the cell surface. Since TbpB exhibits holo-Tf binding specificity, it is possible that this lipoprotein serves to deliver the optimum ligand to TbpA and once the iron has been removed from the ligand, to aid in the release of apo-Tf. This model is supported by the observation that TbpA did not efficiently release Tf in the absence of TbpB. Once iron has been removed from Tf it is necessary to quickly release the apo, iron-depleted ligand, and the C-lobe of TbpB potentially contributes to this task. Since TbpA, unlike TbpB, shows no specificity for holo-Tf (Cornelissen and Sparling 1996), the C-terminus of TbpB may also function to rapidly remove the apo-ligand.

This study highlights the individual roles of the proteins involved in the Tf-iron acquisition system. In our current model, TbpA, although capable of releasing Tf in the absence of TbpB, accomplishes this at a dramatically slower rate. Previous data demonstrated that a TbpA-only strain internalized 50% less iron from Tf as compared to the wild-type strain (Anderson et al. 1994). This result, along with ligand dissociation data from the current study, suggests that the transporter removes iron from Tf but cannot efficiently release the apo-ligand from the cell surface. Therefore, overall iron internalization is reduced in a TbpA-only strain. We conclude that TbpB contributes to increased Tf-iron acquisition efficiency by affecting rapid association and dissociation of the optimum ligand so that multiple rounds of iron internalization can occur.

**Acknowledgments** Funding for this work was provided by Public Health Service grant R01 AI47141 from the National Institute of Allergy and Infectious Diseases, National Institutes of Health. We gratefully acknowledge Dr. Darrell Peterson, VCU Department of Biochemistry, for useful discussions regarding analysis of ligand dissociation data.

## References

- Alcantara J, Schryvers AB (1996) Transferrin binding protein two interacts with both the N-lobe and C-lobe of ovotransferrin. *Microb Pathog* 20(2):73–85. doi:[10.1006/mpat.1996.0007](https://doi.org/10.1006/mpat.1996.0007)
- Anderson JE, Sparling PF et al (1994) Gonococcal transferrin-binding protein 2 facilitates but is not essential for transferrin utilization. *J Bacteriol* 176(11):3162–3170
- Bertani G (1951) Studies on lysogenesis I.: The mode of phage liberation by lysogenic *Escherichia coli*. *J Bacteriol* 62(3):293–300
- Bertani G (2004) Lysogeny at mid-twentieth century: P1, P2, and other experimental systems. *J Bacteriol* 186(3):595–600. doi:[10.1128/JB.186.3.595-600.2004](https://doi.org/10.1128/JB.186.3.595-600.2004)
- Buchanan SK, Smith BS et al (1999) Crystal structure of the outer membrane active transporter FepA from *Escherichia coli*. *Nat Struct Biol* 6(1):56–63. doi:[10.1038/4931](https://doi.org/10.1038/4931)
- Bylund DB, Yamamura HI (1990) Methods for receptor binding. In: Yamamura HI (ed) *Methods in neurotransmitter receptor analysis*. Raven Press Ltd., New York
- Cadieux N, Kadner RJ (1999) Site-directed disulfide bonding reveals an interaction site between energy-coupling protein TonB and BtuB, the outer membrane cobalamin transporter. *Proc Natl Acad Sci USA* 96:10673–10678. doi:[10.1073/pnas.96.19.10673](https://doi.org/10.1073/pnas.96.19.10673)
- Cornelissen CN, Sparling PF (1996) Binding and surface exposure characteristics of the gonococcal transferrin receptor are dependent on both transferrin-binding proteins. *J Bacteriol* 178(5):1437–1444
- Cornelissen CN, Biswas GD et al (1992) Gonococcal transferrin-binding protein 1 is required for transferrin utilization and is homologous to TonB-dependent outer membrane receptors. *J Bacteriol* 174(18):5788–5797
- Cornelissen CN, Anderson JE et al (1997a) Characterization of the diversity and the transferrin-binding domain of gonococcal transferrin-binding protein 2. *Infect Immun* 65(2):822–828
- Cornelissen CN, Anderson JE et al (1997b) Energy-dependent changes in the gonococcal transferrin receptor. *Mol Microbiol* 26(1):25–35. doi:[10.1046/j.1365-2958.1997.5381914.x](https://doi.org/10.1046/j.1365-2958.1997.5381914.x)
- DeRocco AJ, Cornelissen CN (2007) Identification of transferrin-binding domains in TbpB expressed by *Neisseria gonorrhoeae*. *Infect Immun* 75(7):3220–3232. doi:[10.1128/IAI.00072-07](https://doi.org/10.1128/IAI.00072-07)
- Gudmundsdottir A, Bell PE et al (1989) Point mutations in a conserved region (TonB box) of *Escherichia coli* outer membrane protein BtuB affect vitamin B12 transport. *J Bacteriol* 171(12):6526–6533
- Irwin SW, Averil N et al (1993) Preparation and analysis of isogenic mutants in the transferrin receptor protein genes, *tbpA* and *tbpB*, from *Neisseria meningitidis*. *Mol Microbiol* 8(6):1125–1133. doi:[10.1111/j.1365-2958.1993.tb01657.x](https://doi.org/10.1111/j.1365-2958.1993.tb01657.x)
- Jian-Xin Wang HIY, Wang W (1992) The Use of the filtration technique in in vitro radioligand binding assays for membrane-bound and solubilized receptors. In: Hulme EC et al (eds) *Receptor-ligand interactions a practical approach*. Oxford University Press, New York
- Jones SW (1982) Identification of receptors in vitro. In: Eckelman WC (ed) *Receptor-binding radiotracers*, vol 1. CRC Press, Boca Raton, pp 15–36
- Kellogg DS Jr, Peacock WL Jr et al (1963) *Neisseria gonorrhoeae*. I. Virulence genetically linked to clonal variation. *J Bacteriol* 85:1274–1279
- Kenney CD, Cornelissen CN (2002) Demonstration and characterization of a specific interaction between gonococcal transferrin binding protein A and TonB. *J Bacteriol* 184(22):6138–6145. doi:[10.1128/JB.184.22.6138-6145.2002](https://doi.org/10.1128/JB.184.22.6138-6145.2002)
- Klug CS, Eaton SS et al (1998) Ligand-induced conformational change in the ferric enterobactin receptor FepA as studied by site-directed spin labeling and time-domain ESR. *Biochemistry* 37:9016–9023. doi:[10.1021/bi980144e](https://doi.org/10.1021/bi980144e)
- Krell T, Renaud-Mongenie G et al (2003) Insight into the structure and function of the transferrin receptor from *Neisseria meningitidis* using microcalorimetric techniques. *J Biol Chem* 278(17):14712–14722. doi:[10.1074/jbc.M204461200](https://doi.org/10.1074/jbc.M204461200)
- Larsen RA, Foster-Hartnett D et al (1997) Regions of *Escherichia coli* TonB and FepA proteins essential for in vivo physical interactions. *J Bacteriol* 179(10):3213–3221
- Lewis LA, Dyer DW (1995) Identification of an iron-regulated outer membrane protein of *Neisseria meningitidis* involved in the utilization of hemoglobin complexed to haptoglobin. *J Bacteriol* 177(5):1299–1306
- Lissolo L, Maitre-Wilmotte G et al (1995) Evaluation of transferrin-binding protein 2 within the transferrin-binding complex as a potential antigen for future meningococcal vaccines. *Infect Immun* 63(3):884–890
- Mazarin V, Rokbi B et al (1995) Diversity of the transferrin-binding protein Tbp2 of *Neisseria meningitidis*. *Gene* 158:145–146. doi:[10.1016/0378-1119\(95\)00151-U](https://doi.org/10.1016/0378-1119(95)00151-U)
- Mickelsen PA, Sparling PF (1981) Ability of *Neisseria gonorrhoeae*, *Neisseria meningitidis*, and commensal *Neisseria* species to obtain iron from transferrin and iron compounds. *Infect Immun* 33(2):555–564
- Mickelsen PA, Blackman E et al (1982) Ability of *Neisseria gonorrhoeae*, *Neisseria meningitidis*, and commensal *Neisseria* species to obtain iron from lactoferrin. *Infect Immun* 35(3):915–920
- Noto JM, Cornelissen CN (2008) Identification of TbpA residues required for transferrin-iron utilization by *Neisseria gonorrhoeae*. *Infect Immun* 76(5):1960–1969. doi:[10.1128/IAI.00020-08](https://doi.org/10.1128/IAI.00020-08)
- Renaud-Mongenie G, Poncet D et al (1997) Identification of human transferrin-binding sites within meningococcal transferrin-binding protein B. *J Bacteriol* 179(20):6400–6407
- Retzer MD, Yu RH et al (1998) Discrimination between apo and iron-loaded forms of transferrin by transferrin binding protein B and its N-terminal subfragment. *Microb Pathog* 25:175–180. doi:[10.1006/mpat.1998.0226](https://doi.org/10.1006/mpat.1998.0226)

- Retzer MD, Yu RH et al (1999) Identification of sequences in human transferrin that bind to the bacterial receptor protein, transferrin-binding protein B. *Mol Microbiol* 32(1): 111–121. doi:[10.1046/j.1365-2958.1999.01331.x](https://doi.org/10.1046/j.1365-2958.1999.01331.x)
- Rohde KH, Dyer DW (2004) Analysis of haptoglobin and hemoglobin-haptoglobin interactions with the *Neisseria meningitidis* TonB-dependent receptor HpuAB by flow cytometry. *Infect Immun* 72(5):2494–2506. doi:[10.1128/IAI.72.5.2494-2506.2004](https://doi.org/10.1128/IAI.72.5.2494-2506.2004)
- Schryvers AB, Morris LJ (1988) Identification and characterization of the human lactoferrin-binding protein from *Neisseria meningitidis*. *Infect Immun* 56(5):1144–1149
- Scott DC, Newton SMC et al (2002) Surface loop motion in FepA. *J Bacteriol* 184(17):4906–4911. doi:[10.1128/JB.184.17.4906-4911.2002](https://doi.org/10.1128/JB.184.17.4906-4911.2002)
- Sims KL, Schryvers AB (2003) Peptide-peptide interactions between human transferrin and transferrin-binding protein B from *Moraxella catarrhalis*. *J Bacteriol* 185(8):2603–2610. doi:[10.1128/JB.185.8.2603-2610.2003](https://doi.org/10.1128/JB.185.8.2603-2610.2003)
- Vonder Haar RA, Legrain M et al (1994) Characterization of a highly structured domain in Tbp2 from *Neisseria meningitidis* involved in binding to human transferrin. *J Bacteriol* 176(20):6207–6213
- West SE, Sparling PF (1987) Aerobactin utilization by *Neisseria gonorrhoeae* and cloning of a genomic DNA fragment that complements *Escherichia coli fluB* mutations. *J Bacteriol* 169(8):3414–3421
- Yost-Daljev MK, Cornelissen CN (2004) Determination of surface-exposed, functional domains of gonococcal transferrin-binding protein A. *Infect Immun* 72(3):1775–1785. doi:[10.1128/IAI.72.3.1775-1785.2004](https://doi.org/10.1128/IAI.72.3.1775-1785.2004)